CHEMICAL CONSTITUENTS AND NITRIC OXIDE INHIBITORY ACTIVITY FROM THE LEAVES OF *OSMANTHUS FRAGRANS* LOUR.

THÀNH PHẦN HÓA HỌC VÀ HOẠT TÍNH ỨC CHẾ NITRIC OXIDE TỪ LÁ LOÀI *OSMANTHUS FRAGRANS* LOUR.

Le Ba Vinh[1,2], Dinh Thi Thu Phuong[3], Nguyen Cao Cuong[2], Nguyen Ngoc Linh[3,*]

DOI: http://doi.org/10.57001/huih5804.2025.206

ABSTRACT

Osmanthus fragrans Lour. is a medicinal plant widely used in several Asian countries, including Vietnam, China, Japan, and Korea. Traditionally, it has been utilized for treating weakened vision, halitosis, panting, asthma, cough, toothache, stomachache, diarrhea, rheumatism, body pain, and hepatitis, as well as being commonly used in tea. However, no studies have been reported on the chemical constituents or pharmacological effects of *O. fragrans* in Vietnam. A phytochemical study of *O. fragrans* leaves led to the isolation of six compounds (**1–6**). Their structures were unambiguously elucidated using a combination of NMR spectroscopic data and high-resolution electrospray ionization mass spectrometry (HR-ESI-MS). Moreover, the NO inhibitory activity was also examined. This is the first study to investigate the chemical constituents and pharmacological effects of *O. fragrans* collected in Vietnam.

Keywords: *Osmanthus fragrans, chemical constituent, pharmacological effect, medicinal plant, antioxidant.*

TÓM TẮT

Osmanthus fragrans Lour. là một loài dược liệu được sử dụng rộng rãi ở một số quốc gia châu Á, bao gồm Việt Nam, Trung Quốc, Nhật Bản và Hàn Quốc. Theo y học truyền thống, loài cây này được dùng để điều trị suy giảm thị lực, hôi miệng, khó thở, hen suyễn, ho, đau răng, đau dạ dày, tiêu chảy, thấp khớp, đau nhức cơ thể và viêm gan, cũng như được sử dụng phổ biến trong trà. Tuy nhiên, chưa có nghiên cứu nào được báo cáo về thành phần hóa học hoặc tác dụng dược lý của *O. fragrans* tại Việt Nam. Nghiên cứu hóa thực vật trên phần lá loài *O. fragrans* đã phân lập được sáu hợp chất (**1–6**). Cấu trúc của các hợp chất này được xác định một cách rõ ràng thông qua sự kết hợp của dữ liệu phổ NMR và phổ khối ion hóa phun điện phân giải cao (HR-ESI-MS). Thêm vào đó, hoạt tính ức chế sản sinh NO của các hợp chất cũng được đánh giá. Đây là nghiên cứu đầu tiên về thành phần hóa học và tác dụng dược lý của *O. fragrans* thu thập tại Việt Nam.

Từ khóa: *Osmanthus fragrans, thành phần hóa học, hoạt tính dược học, cây thuốc, chất chống oxy hóa.*

[1]Department of Chemistry, University of Bergen, Bergen, Norway
[2]Faculty of Medicine and Pharmacy, Yersin University of Da Lat, Vietnam
[3]Faculty of Pharmacy, Thanh Do University, Vietnam
[*]Email: nnlinh@thanhdouni.edu.vn
Received: 26/02/2025
Revised: 23/5/2025
Accepted: 28/5/2025

1. INTRODUCTION

Natural products derived from herbal medicine have played an important role in drug discovery, serving as the foundation for many clinically approved therapeutics [1]. Over the past few decades, bioactive compounds from plants have significantly contributed to the development of drugs targeting various diseases, including cancer, infectious diseases, neurodegenerative disorders, and metabolic syndromes [2]. The structural diversity and biological complexity of plant-derived secondary metabolites offer unique pharmacophores that synthetic chemistry often struggles to replicate. Despite advances in combinatorial chemistry and high-throughput screening, natural products remain a valuable source for drug discovery, primarily due to their evolutionary optimization for biological interactions. Recent

technological advancements, such as metabolomics, bioinformatics, and synthetic biology, have facilitated the identification, characterization, and modification of plant-derived bioactive molecules. These approaches enhance the potential of natural products in modern drug development, bridging traditional ethnopharmacology with contemporary pharmaceutical sciences [3].

Osmanthus fragrans Lour. (Oleaceae), commonly known as sweet osmanthus, is a traditionally significant medicinal plant widely used in Vietnam, China, Japan, and Korea for the treatment of various ailments, including respiratory disorders, inflammation, and skin conditions [4]. Its fragrant flowers and leaves are also employed in culinary and cosmetic applications, highlighting its cultural and therapeutic importance. To date, phytochemical investigations have identified a diverse range of bioactive secondary metabolites in *O. fragrans*, including flavonoids, terpenes, secoiridoids, and other polyphenolic compounds, which contribute to its broad-spectrum pharmacological properties [5]. Notably, methanol extracts of *O. fragrans* have shown significant antioxidant, anti-inflammatory, cytotoxic, and hepatoprotective effects in experimental studies, indicating its potential for drug development and functional food applications [6]. Given its traditional uses and promising bioactivities, further research on *O. fragrans* is warranted to elucidate its mechanisms of action, isolate novel bioactive compounds, and explore its therapeutic potential in modern medicine [7]. However, there have been no reports regarding the chemical components and their pharmacological effects of *O. fragrans* in Vietnam. Herein, we present the primary study on the secondary metabolites and their anti-inflammatory effects from the leaves of *O. fragrans*.

2. MATERIALS AND METHODS

2.1. General experimental procedures

The Bruker 600MHz NMR spectrometer was used to perform NMR spectra. With chemical shift values (δ) in ppm and coupling constants (J in Hz), TMS was used as an internal standard. Additional data from HSQC, COSY, NOESY, and HMBC studies confirmed structural assignments. A Thermo Fisher LC-LTQ-Orbitrap XL spectrometer (Thermo Fisher, Palo Alto, CA, USA) operating in positive ion mode was used to obtain high-resolution electrospray ionization mass spectrometry (HRESIMS) data. YMC*GEL (ODS-A, 12nm S-150 mm, YMC) and silica gel (Kieselgel 60, 70 - 230 mesh, and 230 - 400 mesh, Merck, Darmstadt, Germany) were utilized for open column chromatography (CC). Merck precoated silica gel 60 F_{254} (1.05554.0001), Sephadex LH-20 (GE Healthcare Bio-Science AB), and RP-C18 F_{254S} plates (1.15685.0001) were used for thin-layer chromatography (TLC). The compounds on the TLC plates were visualized by spraying them with a 10% (v/v) aqueous H_2SO_4 solution and identifying them under UV light (254 and 365nm).

2.2. Plant Material

The leaves of *O. fragrans* was collected from Me Linh, Hanoi in August 2023. The plant was authenticated by Dr. Nguyen Cao Cuong, at the Yersin University, and a voucher specimen (QH 008) has been deposited in the herbarium of the Yersin University, Dalat, Lam Dong, Vietnam.

2.3. Extraction and isolation

The extraction and isolation process in this study was carried out following our previously reported method, with slight modifications [8-10]. Leaves of *O. fragrans* (2.5kg) were extracted with ethanol (EtOH) at room temperature through three consecutive rounds of maceration (5L each). The combined EtOH extracts were concentrated under reduced pressure to afford a crude EtOH residue (450g). This residue was then suspended in water and partitioned sequentially with *n*-hexane and ethyl acetate (EtOAc), yielding *n*-hexane (30g) and EtOAc (120g) fractions, along with an aqueous layer that was reserved for further analysis.

The EtOAc fraction wassubjected to silica gel column chromatography (CC) using a stepwise gradient of $CHCl_3$-MeOH (100:1 to 1:1, v/v), resulting in eight subfractions (E1-E8). Among these, fraction E4 (12g) was further separated by reversed-phase C18 column chromatography (RP-C18 CC) with a isocratic elution of acetone-H_2O (1:2, v/v), yielding compound **4** (3.5mg).

Subfraction E8 (40g) was subjected to silica gel column chromatography using a gradient of $CHCl_3$-MeOH–H_2O (4:1:0.1 to 2:1:0.2, v/v/v) as the mobile phase. The resulting fractions were further purified by Sephadex LH-20 column chromatography using MeOH-H_2O (3:1, v/v), leading to the isolation of compounds **1** (200mg), **2** (98mg), **3** (3.5mg), **4** (9.5 mg), and **6** (1.8mg). Finally, subfraction E7 (12g) was purified by silica gel CC with $CHCl_3$-MeOH-H_2O (7:1:0.01, v/v/v), followed by RP-C18 CC using an acetone-H_2O gradient (1:3 to 2:1, v/v), affording compound **5** (3.8mg).

Compound **1**. White amorphous powder, ^{1}H-NMR (600MHz, CD_3OD) and ^{13}C-NMR (150MHz, CD_3OD), see

Table 1. The data are consisted with the findings in reference [11].

Compound **2**. White amorphous powder, ^{1}H-NMR (600MHz, CD_3OD) δ_H: 4.35 (1H, d, *J* = 8.0Hz, H-1), 3.32 (1H, m, H-2), 3.55 (1H, t, *J* = 9.0Hz, H-3), 3.43 (1H, m, H-4), 3.57 (1H, m, H-5), 4.37 (1H, m, H_a-6), 4.51 (1H, dd, *J* = 12.0, 2.0Hz, H_b-6), 5.20 (1H, s, H-1'), 3.96 (1H, m, H-2'), 3.72 (1H, m, H-3'), 3.41 (1H, m, H-4'), 4.02 (1H, dd, *J* = 9.5, 6.0Hz, H-5'), 1.26 (3H, d, *J* = 6.0Hz, H-6'), 7.05 (1H, d, *J* = 2.0Hz, H-2''), 6.78 (1H, d, *J* = 8.0Hz, H-5''), 6.90 (1H, dd, *J* = 8.0, 1.5Hz, H-6''), 7.57 (1H, d, *J* = 16.0Hz, H-7''), 6.30 (1H, d, *J* = 16.0Hz, H-8''), 6.69 (1H, d, *J* = 2.0Hz, H-2'''), 6.65 (1H, d, *J* = 8.0Hz, H-5'''), 6.55 (1H, dd, *J* = 8.0, 2.0Hz, H-6''), 2.79 (2H, m, H-7''), 3.72 (1H, m, H_a-8'''), 3.96 (1H, m, H_b-8'''); ^{13}C-NMR (150MHz, CD_3OD) δ_C: 104.4 (C-1), 75.7 (C-2), 83.9 (C-3), 70.4 (C-4), 75.4 (C-5), 64.6 (C-6), 102.7 (C-1'), 72.4 (C-2'), 72.2 (C-3'), 74.0 (C-4'), 70.0 (C-5'), 17.9 (C-6'), 127.7 (C-1''), 115.1 (C-2''), 147.2 (C-3''), 149.6 (C-4''), 116.5 (C-5''), 123.2 (C-6''), 146.8 (C-7''), 114.8 (C-8''), 169.1 (C-9''), 131.4 (C-1'''), 117.1 (C-2'''), 146.1 (C-3'''), 144.6 (C-4'''), 116.3 (C-5'''), 121.3 (C-6'''), 36.7 (C-7'''), 72.3 (C-8'''). The data are consisted with the findings in reference [12].

Compound **3**. White amorphous powder, ^{1}H-NMR (600MHz, CD_3OD) δ_H: 4.44 (1H, d, *J* = 8.0Hz, H-1, 5.20 (1H, s, H-1'), 1.11 (3H, d, *J* = 6.0Hz, H-6'), 7.08 (1H, br s, H-2''), 6.86 (1H, d, *J* = 8.5Hz, H-5''), 6.99 (1H, d, *J* = 8.5 Hz, H-6''), 7.61 (1H, d, *J* = 16.0 Hz, H-7''), 6.29 (1H, d, *J* = 16.0Hz, H-8''), 6.80 (1H, br s, H-2'''), 6.73 (1H, d, *J* = 8.0Hz, H-5'''), 6.69 (1H, d, *J* = 8.0Hz, H-6'''), 4.77 (1H, m, H-7'''), 3.59 (2H, m, H-8'''); ^{13}C-NMR (150MHz, CD_3OD) δ_C: 104.5 (C-1), 73.1 (C-2), 83.6 (C-3), 70.5 (C-4), 76.0 (C-5), 62.2 (C-6), 103.0 (C-1'), 72.2 (C-2'), 72.0 (C-3'), 73.7 (C-4'), 70.5 (C-5'), 18.4 (C-6'), 127.6 (C-1''), 114.8 (C-2''), 146.7 (C-3''), 149.7 (C-4''), 116.6 (C-5''), 123.3 (C-6''), 148.2 (C-7''), 115.3 (C-8''), 168.5 (C-9''), 133.6 (C-1'''), 114.7 (C-2'''), 146.2 (C-3'''), 146.1 (C-4'''), 116.3 (C-5'''), 119.2 (C-6'''), 76.6 (C-7'''), 73.5 (C-8'''). The data are consistedwith the findings in reference [13].

Compound **4**. White amorphous powder, ^{1}H-NMR (600MHz, DMSO-d_6) δ_H: 6.77 (1H, s, H-3), 6.19 (1H, d, *J* = 2.0Hz, H-6), 6.48 (1H, d, *J* = 2.0Hz, H-8), 7.92 (2H, d, *J* = 8.5Hz, H-2',6'), 6.92 (2H, d, *J* = 8.5Hz, H-3',5'); ^{13}C-NMR (150MHz, CD_3OD) δ_C: 164.2 (C-2), 102.9 (C-3), 181.8 (C-4), 157.4 (C-5), 94.0 (C-6), 163.8 (C-7), 98.9 (C-8), 161.5 (C-9), 103.7 (C-10), 121.2 (C-1'), 128.5 (C-2', 6'), 116.0 (C-3', 5'), 161.2 (C-4'). The data are consistedwith the findings in reference [14].

Compound **5**. White amorphous powder, ^{1}H-NMR (600MHz, CD_3OD) δ_H: 6.65 (1H, s, H-3), 6.49 (1H, d, *J* = 2.0Hz, H-6), 6.81 (1H, d, *J* = 2.0Hz, H-8), 7.88 (2H, d, *J* = 8.5Hz, H-2',6'), 6.93 (2H, d, *J* = 8.5Hz, H-3',5'), 5.07 (1H, d, *J* = 7.0Hz, H-1''), 3.94 (1H, dd, *J* =12.0, 2.0Hz, H-6α''), 3.72 (1H, dd, *J* =12.0, 6.0Hz, H-6β''); ^{13}C-NMR (150MHz, CD_3OD) δ_C: 166.8 (C-2), 104.1 (C-3), 184.1 (C-4), 163.1 (C-5), 101.2 (C-6), 164.8 (C-7), 96.1 (C-8), 159.0 (C-9), 107.1 (C-10), 123.0 (C-1'), 129.7 (C-2'), 117.1 (C-3'), 162.9 (C-4'), 117.1 (C-5'), 129.7 (C-6'), 101.6 (C-1''), 74.7 (C-2''), 77.9 (C-3''), 71.3 (C-4''), 78.4 (C-5''), 62.5 (C-6''). The data are consistedwith the findings in reference [14].

Compound **6**. White amorphous powder, ^{1}H-NMR (600MHz, CD_3OD) δ_H: 6.64 (1H, s, H-3), 6.44 (1H, br.s, H-6), 6.76 (1H, br.s, H-8), 7.86 (2H, d, *J* = 8.5Hz, H-2',6'), 6.92 (2H, d, *J* = 8.5Hz, H-3',5'), 5.19 (1H, d, *J* = 7.5Hz, H-1''), 5.29 (1H, s, H-1'''), 1.33 (3H, d, *J* = 6.0Hz, H-6'''); ^{13}C-NMR (150MHz, CD_3OD) δ_C: 166.8 (C-2), 104.1 (C-3), 184.0 (C-4), 163.1 (C-5), 101.0 (C-6), 164.4 (C-7), 95.9 (C-8), 159.0 (C-9), 122.9 (C-1'), 129.6 (C-2'), 117.1 (C-3'), 162.9 (C-4'), 117.1 (C-5'), 129.6 (C-6'), 99.8 (C-1''), 79.0 (C-2''), 78.3 (C-3''), 72.2 (C-4''), 79.1 (C-5''), 62.4 (C-6''), 102.5 (C-1'''), 72.2 (C-2'''), 71.4 (C-3'''), 74.0 (C-4'''), 70.0 (C-5'''), 18.3 (C-6'''). The data are consisted with the findings in reference [15].

2.4. Assay for NO inhibitory activity

The American Type Culture Collection (ATCC) provided the murine macrophage cell line RAW 264.7 (TIB-71, ATCC, Manassas, VA, USA). The previously established method was used to perform the NO test [16]. In brief, 96-well plates were cultivated using RAW 264.7 cells (1×10^5 cells/well) for 24 hours. Before being treated with LPS (0.1µg/mL) for 24 hours, cells were pre-treated with samples for 1 hour. An equivalent volume of Griess reagent was combined with 100 µL of cell culture supernatants. After samples were incubated for 24 hours, cell cytotoxicity was assessed using the MTT test [16]. Dexamethasone was used as positive control.

2.5. Molecular docking simulation

The molecular docking simulation was performed following a protocol adapted from previous studies, with minor adjustments [10]. The crystal structures of the iNOS (PDB: 4UX6) and COX-2 (PDB: 6COX) receptor complexes were retrieved from the Protein Data Bank (http://www.rcsb.org/pdb) for the *in silico* analysis. The protein structures were refined using the "Orthogonal Partial Least Squares 4" (OPLS4) potential energy function

and the protein preparation tool in Maestro v12.4 (Schrödinger, New York, NY, USA), until the root-mean-square deviation (RMSD) of non-hydrogen atoms reached a value of 0.3Å. To generate the 2D structures of the 13 ligands, we utilized ChemDraw software 20.0 (PerkinElmer Informatics, Waltham, MA, USA). These 2D structures were subsequently converted to 3D forms using the LigPrep tool (Schrödinger), with each ligand's structure being optimized at a pH of 7.0 ± 2.0. The 3D models of the ligands maintained their chirality, and their energy was minimized using the OPLS4 force field in the final step of LigPrep. For the receptor grid generation, we employed the Receptor Grid Generation tool in Maestro v12.4 (NM share, version 6.0.134; Schrödinger) to create the docking grid for the receptor's active site, based on the coordinates obtained from the PDB file. The grid was positioned at the location of the co-crystallized ligand. The active site was defined by the coordinates X, Y, and Z, which were 38.31, -39.24, and 12.96 for 4UX6, and 45.87, -22.15, and 8.34 for 6COX, respectively The grid box dimensions were adjusted to match the size of the co-crystallized ligand, with dimensions set to 20 × 20 × 20Å^3. For the docking process, Glide was used in extra precision (XP) mode to perform the calculations.

3. RESULTS AND DISCUSSION

The EtOH extract of *O. fragrans* was partitioned based on increasing polarity using *n*-hexane and ethyl acetate (EtOAc). The EtOAc fraction was subjected to chromatographic separation techniques to obtain six compounds (**1–6**) through repeated column chromatography (CC) on silica gel, RP-C18, and Sephadex LH-20. Separately, the ethanolic extract of O. fragrans leaves was fractionated with *n*-hexane, ethyl acetate, and water, respectively. Using a combination of chromatographic techniques (silica gel, RP-C18, Sephadex LH-20, and HPLC), compounds **1–6** were purified. Based on a comprehensive analysis of spectroscopic data and comparison with previously reported data, the chemical structures of the isolated compounds were identified as acteoside (**1**), isoacteoside (**2**), hydroxyacteoside (**3**), apigenin (**4**), apigenin 7-*O*-glucoside (**5**), and apigenin 7-*O*-neohesperidoside (**6**).

Compound **1** was obtained as a white amorphous powder. The molecular formula was determined to be $C_{29}H_{36}O_{15}$ based on HR-ESI-MS analysis ([M-H]$^-$, *m/z* 623.1969; calcd 623.1981). Analysis of the ^{1}H NMR spectrum of compound **1** revealed six aromatic resonances at δ_H 7.07 (1H, d, *J* = 2.0Hz, H-2''); 6.79 (1H, d, *J* = 8.0Hz, H-5''); 6.96 (1H, dd, *J* = 8.0, 2.0Hz, H-6''); 6.71 (1H, d, *J* = 2.0Hz, H-2'''); 6.69 (1H, d, *J* = 8.0Hz, H-5'''); and 6.57 (1H, dd, *J* = 8.0, 2.0Hz, H-6''). Additionally, there are a pair of olefinic protons at δ_H 7.60 (1H, d, *J* = 16.0Hz, H-7'') and 6.29 (1H, d, *J* = 16.0Hz, H-8''). Methylene protons were observed at δ_H 2.80 (2H, dd, *J* = 13.0, 6.7 Hz, H-7'''), 3.73 (1H, m, H_a-8'''), and 4.06 (1H, ddd, *J* = 9.5, 8.5, 7.0Hz, H_b-8'''). Consistent with these observations, the ^{13}C NMR and HSQC spectra exhibited 28 carbon resonances, consisting of one methyl, three methylenes, ten methines (nine of which are oxygenated), and seven quaternary carbons (one olefinic at δ_C 168.3). These NMR data suggest that the structure of compound **1** contains features characteristic of caffeic acid, glucose, and rhamnose moieties. The planar structure was deduced from HMBC cross-peaks. In particular, the HMBC correlation from H-1 (δ_H 4.39, 1H, d, *J* = 8.0Hz) to C-8''' (δ_C 72.2ppm) and from H-1' (δ_H 5.20, 1H, d, *J* = 1.5Hz) to C-3 (δ_C 81.6ppm) verified the linkage of the two anomeric positions of Glc and Rham. By comparing the NMR data of compound **1** with verbascoside, we found completely identical values [11]. Therefore, the structure of compound **1** was determined to be verbascoside.

Compounds **2** and **3** were also isolated as amorphous powders. Their structures were elucidated based on detailed NMR spectroscopic analyses. A comparison of the spectral data of compounds **1** and **2** revealed slight differences, particularly at the C-6 and C-9″ positions. In the ^{1}H and ^{13}C NMR spectra of compound **2**, the chemical shifts were observed to move downfield, from δ_C 62.3 to 64.6 (C-6) and from δ_C 168.3 to 169.1 (C-9″), respectively. These changes suggest that the caffeic acid moiety is attached at the C-6 position in compound **2**. Additionally, a comparison of the NMR data of compound 2 with previously reported literature values confirmed that its structure is identical to that of isoacteoside. Similarly, a comparison of the NMR data of compounds **1** and **3** revealed the absence of a methylene group and the appearance of a methine signal. This observation suggests that the structure of compound **3** is similar to that of compound **1**, but with a hydroxyl group substituted at the C-7''' position. The structure of compound 3 was determined to be campneoside II based on a comparison of its NMR data with previously reported literature values.

Compound **4** was obtained as a yellow amorphous powder. The ^{1}H and ^{13}C NMR spectra indicated that compound **4** is a flavonoid, showing characteristic

aromatic proton resonances at δ_H 6.19 (1H, d, *J* = 1.9Hz, H-6), 6.48 (1H, d, *J* = 1.9Hz, H-8), 7.92 (2H, d, *J* = 8.7Hz, H-2', 6'), 6.92 (2H, d, *J* = 8.7Hz, H-3', 5'), and corresponding carbon signals at δ_C 94.0 (C-6), 98.9 (C-8), 128.5 (C-2', 6'), and 116.0 (C-3', 5'), consistent with a flavonoid skeleton. Additionally, a comparison of the NMR data of compound 4 with previously reported literature values confirmed that it was identified as apigenin.

Compounds **5** and **6** were also isolated as yellow amorphous powders. The ^{1}H and ^{13}C NMR spectra of compound **5** indicated that it is similar to compound **4**; however, the presence of a sugar moiety attached at the C-7 position was evident, with characteristic chemical shifts at δ_C 101.6 (C-1''), 74.7 (C-2''), 77.9 (C-3''), 71.3 (C-4''), 78.4 (C-5''), and 62.5 (C-6''). In contrast, the ^{1}H and ^{13}C NMR data for compound **6** revealed the presence of two sugar

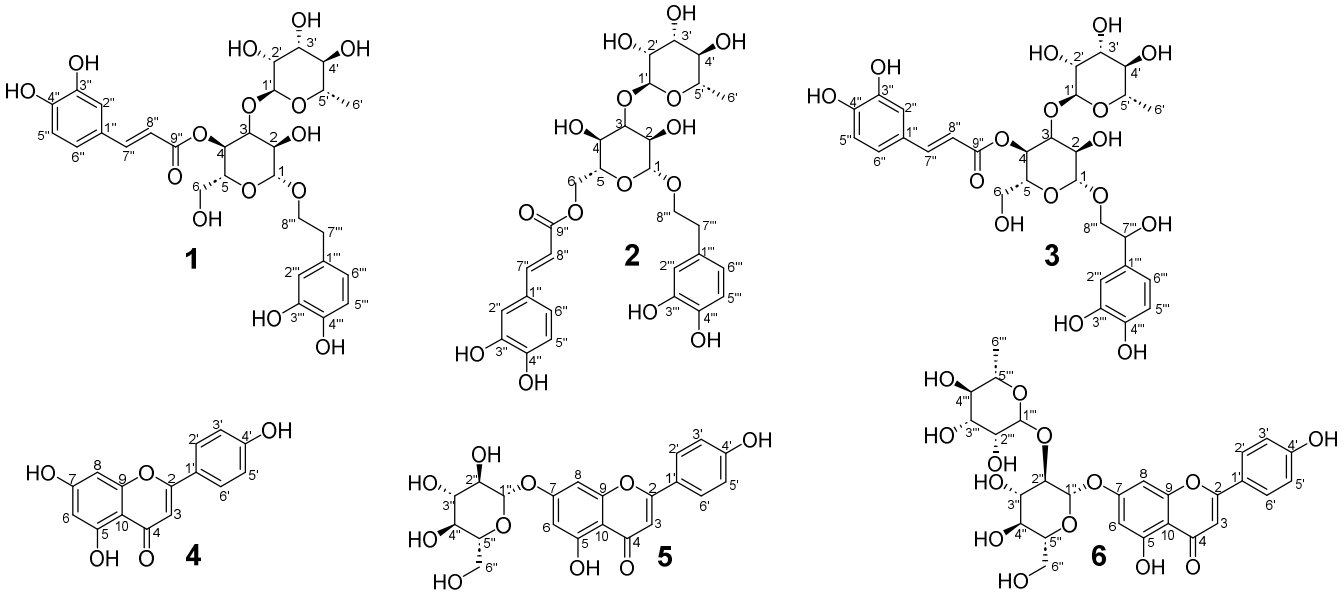

Figure 1. Compounds **1-6** isolated from the leaves of *O. fragrans*

Table 1. ^{1}H (600MHz) [ppm, Mult, (*J* in Hz)] and ^{13}C NMR (150MHz) spectroscopic data of compound **1**

Position	δ_C	δ_H (mult., *J* in Hz)		δ_C	δ_H(mult., *J* in Hz)
1	104.2	4.39 (1H, d, *J* = 8.0Hz)	4″	149.8	-
2	76.0	3.40 (1H, dd, *J* = 9.0, 8.0Hz)	5″	116.5	6.79 (1H, d, *J* = 8.0Hz)
3	81.6	3.83 (1H, t, *J* = 9.0Hz)	6″	123.2	6.96 (1H, dd, *J* = 8.0, 2.0Hz)
4	70.6	4.93 (1H, t, *J* = 9.5Hz)	7″	148.0	7.60 (1H, d, *J* = 16.0Hz)
5	76.2	3.54 (1H, m)	8″	114.7	6.29 (1H, d, *J* = 16.0Hz)
6	62.3	3.54 (1H, m), 3.63 (1H, d, *J* = 10.0Hz)	9″	168.3	-
1′	103.0	5.20 (1H, d, *J* =1.5Hz)	1‴	131.5	-
2′	72.3	3.93 (1H, dd, *J* = 3.0, 2.0Hz)	2‴	117.1	6.71 (1H, d, *J* = 2.0Hz)
3′	70.4	3.59 (1H, m)	3‴	146.1	-
4′	73.8	3.30 (1H, m)	4‴	144.7	-
5′	72.0	*	5‴	116.3	6.69 (1H, d, *J* = 8.0Hz)
6′	18.4	1.10 (3H, d, *J* = 6.0Hz)	6‴	121.3	6.57 (1H, dd, *J* = 8.0, 2.0Hz)
1″	127.6	-	7‴	36.5	2.80 (2H, dd, *J* = 13.0, 6.5Hz)
2″	115.2	7.07 (1H, d, *J* = 2.0Hz)	8‴	72.2	3.73 (1H, m), 4.06 (1H, ddd, *J* = 9.5, 8.5, 7.0Hz)
3″	146.8	-			

Assignments were done by HSQC and HMBC experiments.

**Overlapped signals.*

moieties. By comparing the NMR data with previously reported values, compounds **5** and **6** were identified as apigenin 7-*O*-glucoside and rhoifolin, respectively.

Nitric oxide (NO) is one of the key mediators involved in inflammatory responses and pathogenesis. Numerous studies have reported that secondary metabolites from *O. fragrans* exhibit strong anti-inflammatory effects. Therefore, we investigated the inhibitory effects of isolated compounds from *O. fragrans* on LPS-stimulated NO production in RAW264.7 cells. Without exhibiting cytotoxicity, only compound **1** showed significant inhibition of NO production in LPS-activated macrophages, with an IC_{50} value of $9.48 \pm 0.22\mu M$, compared to the positive control dexamethasone, which had an IC_{50} value of $6.56 \pm 0.25\mu M$.

Molecular docking simulation is a cost-effective and efficient tool widely used in drug discovery. By simulating the interaction between compounds and target proteins, it enables the identification of promising candidates for further experimental validation. In this study, based on in vitro screening results, compound **1** was selected for further investigation to explore its underlying mechanisms of anti-inflammatory activity. This compound demonstrated significant potential in modulating key inflammatory pathways, making it a candidate for more in-depth mechanistic studies.

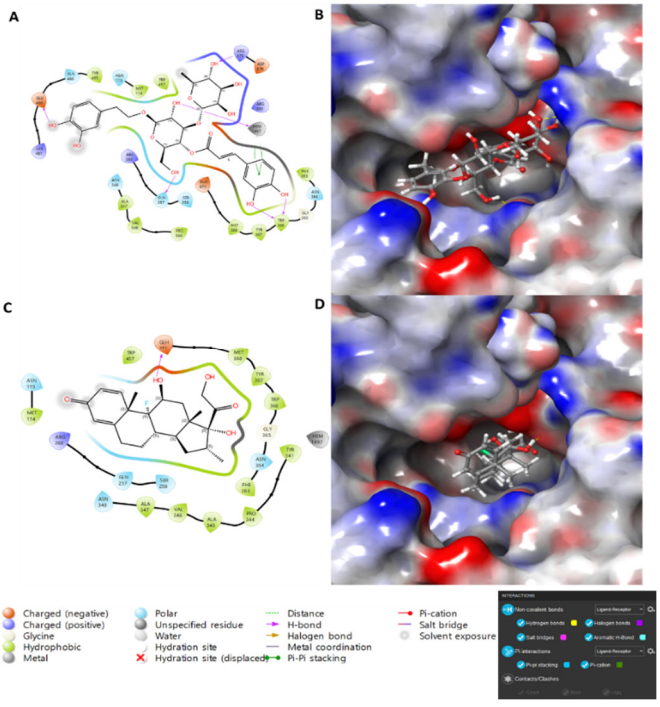

Figure 2. Molecular docking simulations (A-D) showing the binding interactions of compound **1** and dexamethasone (used as a positive control) with iNOS (PDB: 4UX6), visualized in both 2D and 3D formats

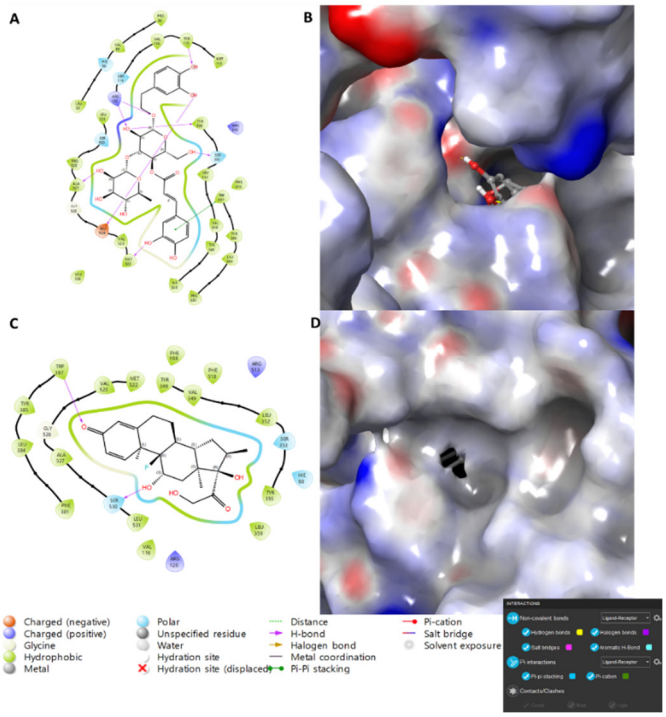

Figure 3. Molecular docking simulations (A-D) illustrating the interactions between compound **1** and dexamethasone (positive control) with COX-2 (PDB: 6COX), also presented through both 2D and 3D visualizations.

Inducible nitric oxide synthase (iNOS) and cyclooxygenase-2 (COX-2) are critical enzymes involved in the inflammatory response, playing essential roles in the production of inflammatory mediators like nitric oxide (NO) and prostaglandins. As such, targeting iNOS and COX-2 has become a promising therapeutic approach for inflammatory disorders. Understanding the molecular mechanisms that regulate iNOS and COX-2 expression and activity is crucial for the development of effective interventions aimed at controlling inflammation and mitigating related pathological conditions. Molecular docking technology is widely utilized in drug development to investigate the interactions between potential inhibitors and target proteins. The crystal structures of iNOS (4UX6) and COX-2 (6-COX) are available in the Protein Data Bank (PDB), revealing detailed information about their active sites, key interactions, and the mechanisms through which inhibitors act on inflammation. Compound **1**, identified as the most potent, was docked into the active sites of both iNOS and COX-2 proteins using the same docking procedure. The results showed that compound **1** binds to the active sites of iNOS and COX-2 with docking scores of -10.566 and -11.733kcal/mol, respectively, compared to dexamethasone with scores of -12.866 and -14.629. In the case of iNOS, the ester group of compound **1** formed

hydrogen bonds with GLN257, TRP366, ARG375, GLU488, and HEM1497 in the active site (Figure 2). In addition, residues such as TYR115, ARG120, SER353, MET522, GLU524, and ALA527 were identified as key players in stabilizing the active conformation of COX-2 (Figure 3). These findings suggest that compound **1** may have potential for further development in treating inflammatory disorders.

4. CONCLUSION

In summary, our ongoing phytochemical investigation of *O. fragrans* has led to the isolation of six compounds (**1–6**). Their structures were identified based on 1D and 2D NMR and HR-ESI-MS data. This is the first study on chemical constituents and their pharmacological effects from the *O. fragrans* collected in Vietnam. The NO inhibitory activity was also examined. In particular, compound **1** exhibited significant inhibition of NO production in LPS-activated macrophages without showing cytotoxicity, with an IC_{50} value of 9.48 ± 0.22 μM. For comparison, the positive control dexamethasone showed an IC_{50} value of 6.56 ± 0.25 μM. Moreover, the underlying mechanisms inflammatory effects of isolated compounds were studied based on molecular docking simulation. These results suggest that the bioactive compounds from the leaves of *O. fragrans* may have significant potential for anti-inflammatory effects.

REFERENCES

[1]. Atanasov A. G., Zotchev S. B., Dirsch V. M., Supuran C. T., "Natural products in drug discovery: advances and opportunities", *Nature reviews drug discovery*, 20, 3, 200-216, 2021.

[2]. Newman D. J., Cragg G. M., "Natural products as sources of new drugs over the 30 years from 1981 to 2010," *Journal of natural products*, 75, 3, 311-335, 2012.

[3]. Thomford N. E., Senthebane D. A., Rowe A., Munro D., Seele P., Maroyi A., Dzobo K., "Natural products for drug discovery in the 21st century: innovations for novel drug discovery," *International journal of molecular sciences*, 19, 6, 1578, 2018.

[4]. Wang B., Luan F., Bao Y., Peng X., Rao Z., Tang Q., Zeng N., "Traditional uses, phytochemical constituents and pharmacological properties of Osmanthus fragrans: A review," *Journal of ethnopharmacology,* 293, 115273, 2022.

[5]. Hung C.Y., Tsai Y.C., Li K.Y., "Phenolic antioxidants isolated from the flowers of Osmanthus fragrans," *Molecules*, 17, 9, 10724-10737, 2012.

[6]. Mao S., Wang K., Lei Y., Yao S., Lu B., Huang W., "Antioxidant synergistic effects of Osmanthus fragrans flowers with green tea and their major contributed antioxidant compounds," *Scientific reports*, 7, 1, 46501, 2017.

[7]. Wang L.M., Li M.T., Jin W.W., Li S., Zhang S.Q., Yu L.J., "Variations in the components of *Osmanthus fragrans* Lour. essential oil at different stages of flowering," *Food chemistry*, 114, 1, 233-236, 2009.

[8]. Vinh L. B., Heo M., Phong N. V., Ali I., Koh Y. S., Kim Y. H., Yang S. Y., "Bioactive compounds from *Polygala tenuifolia* and their inhibitory effects on lipopolysaccharide-stimulated pro-inflammatory cytokine production in bone marrow-derived dendritic cells," *Plants*, 9, 9, 1240, 2020.

[9]. Vinh L. B., Jang H.J., Phong N. V., Cho K., Park S. S., Kang J. S., Kim Y. H., Yang S. Y., "Isolation, structural elucidation, and insights into the anti-inflammatory effects of triterpene saponins from the leaves of *Stauntonia hexaphylla*," *Bioorganic & medicinal chemistry letters*, 29, 8, 965-969, 2019.

[10]. Vinh L. B., Shin S. H., Han Y. K., Kim Y. J., Cuong N. C., Oh S., Lee K. Y., "Identification of interleukin (IL)-33 inhibitory constituents from *Canavalia gladiata* pods," *Antioxidants*, 13, 7, 767, 2024.

[11]. Andary C., Wylde R., Laffite C., Privat G., Winternitz F., "Structures of verbascoside and orobanchoside, caffeic acid sugar esters from *Orobanche rapum-genistae*," *Phytochemistry*, 21, 5, 1123-1127, 1982.

[12]. Li L., Tsao R., Liu Z., Liu S., Yang R., Young J. C., Zhu H., Deng Z., Xie M., Fu Z., "Isolation and purification of acteoside and isoacteoside from *Plantago psyllium* L. by high-speed counter-current chromatography," *Journal of chromatography A*, 1063, 1-2, 161-169, 2005.

[13]. Kang K. H., Jang S. K., Kim B. K., Park M. K., "Antibacterial phenylpropanoid glycosides from *Paulownia tomentosa* Steud," *Archives of pharmacal research*, 17, 470-475, 1994.

[14]. Tavakoli S., Khalighi-Sigaroodi F., Khosravi Dehaghi N., Yaghoobi M., Hajiaghaee R., Gholami A., Ghafarzadegan R., "Isolation and purification of apigenin, quercetin and apigenin 7-O-glycoside from *Apium graveolens* L., *Petroselinum crispum* (Mill.) Fuss, *Allium cepa* L., respectively," *Journal of medicinal plants*, 21, 83, 72-86, 2022.

[15]. Djoukeng J. D., Arbona V., Argamasilla R., Gomez-Cadenas A., "Flavonoid profiling in leaves of citrus genotypes under different environmental situations," *Journal of agricultural and food chemistry*, 56, 23, 11087-11097, 2008.

[16]. Su X. D., Jang H. J., Wang C. Y., Lee S. W., Rho M. C., Kim Y. H., Yang S. Y., "Anti-inflammatory potential of saponins from *Aster tataricus* via NF-κB/MAPK activation," *Journal of natural products,* 82, 5, 1139-1148, 2019.

THÔNG TIN TÁC GIẢ

Lê Bá Vinh[1,2], Đinh Thị Thu Phương[3], Nguyễn Cao Cường[2], Nguyễn Ngọc Linh[3]

[1]Khoa Hóa, Trường Đại học Bergen, Na Uy

[2]Khoa Dược, Trường Đại học Yersin

[3]Khoa Dược, Trường Đại học Thành Đô